Lawrence Berkeley National Laboratory

Title

Field Application of 238U/235U Measurements To Detect Reoxidation and Mobilization of U(IV)

Permalink

https://escholarship.org/uc/item/0sb8m148

Journal

ISSN

Authors

Jemison, Noah E
Shiel, Alyssa E
Johnson, Thomas M
et al.

Publication Date

2018-03-20

DOI

Peer reviewed

Field Application of ^{238}U/^{235}U Measurements To Detect Reoxidation and Mobilization of U(IV)

Noah E. Jemison*[†], Alyssa E. Shiel[‡], Thomas M. Johnson[†], Craig C. Lundstrom[†], Philip E. Long[§], and Kenneth H. Williams[§]

[†] Department of Geology, University of Illinois at Urbana−Champaign, 3081 Natural History Building, 1301 W. Green St., Urbana, Illinois 61801, United States

[‡] College of Earth, Ocean, and Atmospheric Sciences, Oregon State University, 104 CEOAS Administration Building, 101 SW 26th St., Corvallis, Oregon 97331, United States

[§] Earth Sciences Division, Lawrence Berkeley National Laboratory, 1 Cyclotron Road, Berkeley, California 94720, United States

*E-mail jemison2@illinois.edu (N.E.J.).

Abstract

Biostimulation to induce reduction of soluble U(VI) to relatively immobile U(IV) is an effective strategy for decreasing aqueous U(VI) concentrations in contaminated groundwater systems. If oxidation of U(IV) occurs following the biostimulation phase, U(VI) concentrations increase, challenging the long-term effectiveness of this technique. However, detecting U(IV) oxidation through dissolved U concentrations alone can prove difficult in locations with few groundwater wells to track the addition of U to a mass of groundwater. We propose the ^{238}U/^{235}U ratio of aqueous U as an independent, reliable tracer of U(IV) remobilization via oxidation or mobilization of colloids. Reduction of U(VI) produces ^{238}U-enriched U(IV), whereas remobilization of solid U(IV) should not induce isotopic fractionation. The incorporation of remobilized U(IV) with a high ^{238}U/^{235}U ratio into the aqueous U(VI) pool produces an increase in ^{238}U/^{235}U of aqueous U(VI). During several injections of nitrate to induce U(IV) oxidation, ^{238}U/^{235}U consistently increased, suggesting ^{238}U/^{235}U is broadly applicable for detecting mobilization of U(IV).
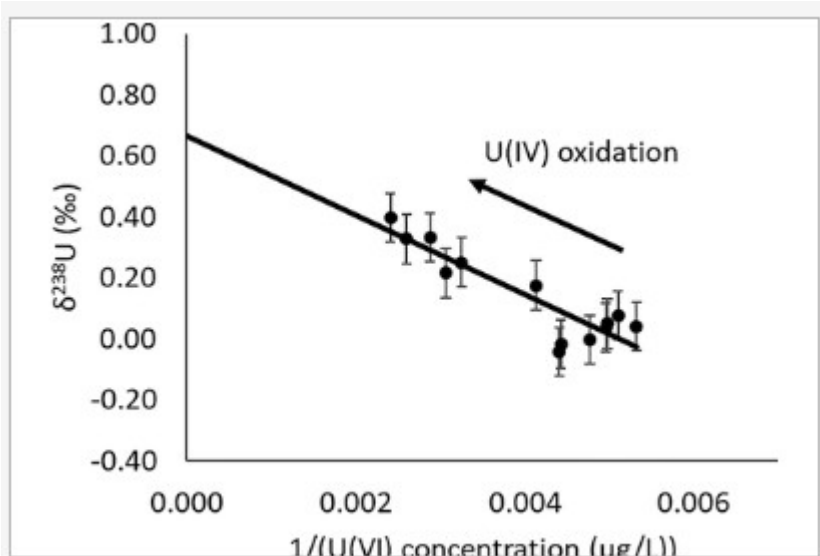
Introduction

Decades of extraction and processing of uranium (U) ore associated with increased demand during World War II and the Cold War has left many sites around the world contaminated with U.[1] A primary concern is U contamination of sediments and groundwater at U mining and milling sites. Uranium is a persistent contaminant in the subsurface at U.S. Department of Energy (DOE) sites particularly in the western U.S.[2] In these systems, U is mobile in its oxidized state, U(VI), but relatively immobile and thus less dangerous in its reduced state, U(IV).[3,4] Through reduction of U(VI) to U(IV), aqueous U concentrations decrease in contaminated aquifers.

Biostimulation has proven to be an effective technique for decreasing U contamination in groundwater.[5−7] Aided by injection of an organic electron donor into the groundwater, microbes reduce U(VI) to U(IV).[5,6,8] Biostimulation also promotes reduction of Fe(III) oxides and sulfate, producing Fe(II) sulfides along with U(IV).[5−7] U(IV) and Fe(II) sulfides are sequestered within the biostimulated reduced zone (BRZ). Some U(IV) associated with microscopic colloids may be transported in groundwater under certain conditions.[9,10] The presence of Fe(II) sulfides can protect U(IV) from oxidation by reacting with oxidants and decreasing their concentrations and thus the oxidation rate of U(IV).[11−15]

If oxidation of sequestered U(IV) occurs following biostimulation, the viability of this technique comes into question. U(IV) can be oxidized by nitrate, nitrite, and dissolved O_2 (DO).[12,14,16−18] U(IV) oxidation by DO occurs abiotically.[12,14] In contrast, U(IV) oxidation by nitrate appears to be primarily a microbial process.[16−18] Nitrite, produced by microbial reduction of nitrate, may also abiotically oxidize U(IV),[16] but this process appears slow,[14] so U(IV) oxidation by nitrite may be aided by microbial activity as well.

U(VI) concentrations are often utilized to track U geochemical processes, but detecting these reactions through U(VI) concentrations alone is difficult in the field and can lead to erroneous conclusions. At many U-contaminated sites, few wells are available for groundwater sampling, and researchers cannot reliably track masses of groundwater as they advect downstream. With a well-instrumented field site, the removal of U(VI) from groundwater by biostimulation can be evaluated by monitoring U(VI) concentrations downstream of the electron donor injection and comparing them to upstream values.[6] However, even in well-characterized sites, some geochemical reactions are still difficult to parse with U(VI) concentrations alone. For example, an observed increase in U(VI) concentration downstream of the injection wells following a biostimulation may result from the advection of U(VI) from upstream, desorption of adsorbed U(VI), and reoxidation of U(IV) produced by the biostimulation. Here we evaluate $^{238}U/^{235}U$ ratios as an independent geochemical tool for detecting U(IV) oxidation.

The two most abundant isotopes of U, ^{238}U and ^{235}U, have half-lives of 4.47×10^9 and 0.70×10^9 years, respectively,[19] and may be treated as stable over short time scales such as those considered here. Variations in the relative abundances are quantified by measuring $^{238}U/^{235}U$ ratios, which are conveniently reported as a per mil deviation from that of the U isotopic standard CRM 112-A:

$$\delta^{238}U = \left[\frac{(^{238}U/^{235}U)_{sample}}{(^{238}U/^{235}U)_{CRM\ 112-A}} - 1 \right] \times 1000\text{‰} \qquad (1)$$

Microbial reduction has been shown to fractionate U isotopes, with the U(IV) product isotopically heavy (i.e., having relatively high $^{238}U/^{235}U$) and the remaining U(VI) becoming isotopically light as reduction proceeds.[20−23] Abiotic U(VI) reduction has been observed to induce little to no isotopic fractionation in some studies.[21,24] However, a recent study[25] of abiotic U(VI) reduction with Fe(II) sulfides in an aqueous matrix similar to those of natural settings detected isotopic fractionation with a magnitude similar to that of microbial U(VI) reduction. Adsorption of aqueous U(VI) results in small $^{238}U/^{235}U$ shifts, with adsorbed U(VI) isotopically light.[26−29] The process of oxidizing solid U(IV) should result in little to no isotopic fractionation (further explanation in the Supporting Information).[30] Oxidizing U(IV) previously deposited via reduction (enriched in ^{238}U) and releasing it to solution should increase the $\delta^{238}U$ value of aqueous U(VI). Measurement of $\delta^{238}U$ in groundwater has potential to detect U(IV) oxidation and aid in the assessment of the long-term stability of U(IV) in a variety of environmental settings.

To examine the relationship between U(IV) oxidation and $^{238}U/^{235}U$ ratios in a field setting, we conducted two successive oxidation experiments in 2013 and 2016. These experiments were carried out in a plot where extensive deposition of U(IV) had been previously induced by biostimulated U(VI)

reduction.(7,23) In our experiments, nitrate was injected into the subsurface to induce oxidation of U(IV). Using the results of these field experiments, we sought to evaluate $^{238}U/^{235}U$ ratios as a tool for detecting reoxidation of U(IV) produced by biostimulation and thus the potential to assess the long-term viability of biostimulation as a remedial strategy.

Methods

Previous Biostimulation Experiments

This study focuses on the site of a former U mill in Rifle, CO, with U-contaminated groundwater (~200 µg/L U(VI)) within a sandy gravel alluvial aquifer (detailed site characteristics in the Supporting Information).(6,7) In consecutive years, 2010–11 and 2011–12, biostimulation experiments were carried out in an array of monitoring and injection wells known as plot C (Figure 1). Core samples and geophysical surveying of plot C prior to acetate amendment demonstrated that this area contained low amounts of organic carbon and Fe(II) sulfides.(31) Some differences in permeability and distribution of Fe(III) oxides have been observed within plot C, which likely affected rates of sulfate and U(VI) reduction.(32,33) In the first year, acetate (50 mM within injection tank) was injected across the entire plot through ten injection wells, CG-01 to CG-10, for 23 days (Figure 1).(7,23) Bicarbonate (50 mM) was also injected in the western half of the plot in wells CA-01 to CA-03, upstream of wells CG-07 to CG-09 to desorb adsorbed U(VI) (Figure 1).(7,34) In the second experiment, acetate was injected at a higher concentration (150 mM) for a longer period (72 days) to induce greater sulfate and U(VI) reduction. This injection of acetate was restricted to the eastern half of plot C through wells CG-01 to CG-05 (Figure 1).(23) During both biostimulation experiments, U(VI) concentrations in the downstream wells decreased below the EPA maximum contaminant level of 30 µg/L.(7) In addition, $\delta^{238}U$ measured in downstream monitoring wells during the biostimulation experiments decreased significantly due to preferential reduction of ^{238}U.(23)
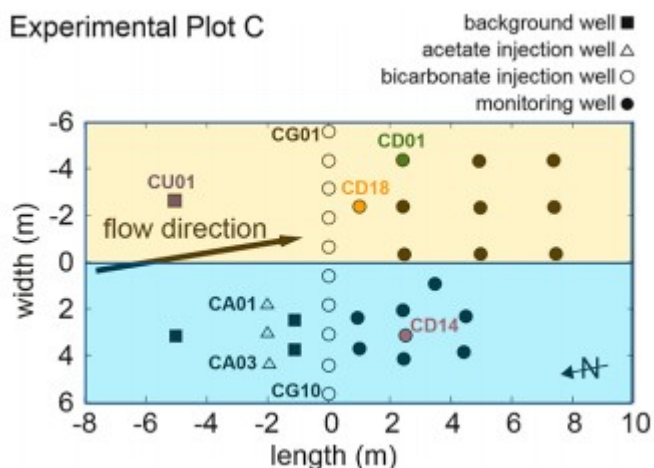
Figure 1. Location of wells in plot C. Bicarbonate was injected in wells CA-01 to CA-03 and acetate in CG-06 to CG-10 in blue. More acetate was injected into wells CG-01 to CG-05 in yellow, inducing more production of Fe(II) sulfides and U(IV).

Oxidation Experiments

Following the biostimulation experiments described above, two oxidation experiments using nitrate were performed in plot C (Table S1 and Figure 1). The first experiment was conducted in fall 2013, approximately two years after the second acetate injection ceased. In a storage tank, groundwater was amended with sodium nitrate (2.9 mM after mixing) and deuterium enriched water (δD = 210.8‰ after mixing) as a tracer.[35] This groundwater was injected into the eastern half of plot C through wells CG-01 to CG-05 (Table S1 and Figure 1). Therefore, only the eastern half of the biostimulation plot was subjected to this oxidation event. The amended groundwater was injected at a rate of 36 mL/min/well for 23 days, producing nitrate groundwater concentrations of 0.5 mM at the injection wells (Table S1).[35] Then, the injection rate was increased to 120 mL/min/well for 11 days to increase the rate of U(IV) oxidation, producing nitrate concentrations of 2 mM at the injection wells. Cross-well mixing was conducted to homogenize nitrate groundwater concentrations across the injection area. [35] Groundwater was collected by a peristaltic pump from upstream well CU-01 and downstream wells CD-18 and CD-01, ~1.0 and ~2.5 m away from the injection well, respectively (Figure 1). Groundwater was collected over a period of four months, capturing both the increase in U(VI) concentrations associated with U(IV) oxidation and the decrease in U(VI) concentrations after the injection ended and nitrate levels in the plot returned to normal.

The second nitrate injection was conducted in fall 2016, approximately five years after the second acetate injection ceased. Groundwater from well CU-01 was added to a gas-impermeable bag and amended with sodium nitrate (44 mM after mixing) and potassium bromide (22 mM after mixing) as a tracer. The nitrate-amended groundwater was injected on both sides of plot C into wells CG-01 to CG-03 and CG-07 to CG-09 for a period of 5 days (Table S1 and Figure 1). Groundwater was injected at a rate of 15 mL/min/well to produce nitrate concentrations of 3 mM at the injection wells, higher than the first oxidation experiment (Table S1). Cross-well mixing was utilized to produce consistent oxidizing fronts across the eastern half of plot C from CG-01 to CG-03 and across the western half from CG-07 to CG-09. Groundwater was collected from upstream well CU-01 and downstream wells CD-01 and CD-14 to capture the oxidizing front from the eastern and western halves of plot C, respectively (Figure 1). Groundwater was collected over a period of 22 days, capturing the increase in dissolved U concentrations associated with the onset of U(IV) oxidation.

We performed oxidation experiments on both the eastern and western halves of plot C, which had undergone distinct biostimulation treatments, to examine the consistency of the isotopic response to U(IV) oxidation, despite differences in the amount and distribution of U(IV). Both biostimulation

experiments (in 2010–11 and 2011–12) had injected acetate in the eastern half of plot C, likely resulting in substantial amounts of U(IV) and Fe(II) sulfides downstream of the injection wells. Acetate was injected in the western half of plot C only in the 2010–11 biostimulation experiment, which involved less acetate and thus less U(VI) and sulfate reduction than the 2011–12 experiment. In addition, the western half was affected by the injection of bicarbonate to induce desorption of U(VI) in 2010–11. The differences in the conditions induced between the two sides of plot C produced distinct quantities and distributions of U(IV) and Fe(II) sulfides downstream of the injection wells. By comparing the change in $\delta^{238}U$ induced by oxidation of U(IV) on the western half of plot C to the eastern half, the broad applicability of $\delta^{238}U$ for detecting U(IV) oxidation may begin to be assessed. If a consistent change in $\delta^{238}U$ is seen, this would suggest that $\delta^{238}U$ may be applied at multiple U-contaminated sites for identifying U(IV) oxidation from BRZ's with varying treatments for inducing reduction.

In addition, the eastern half of plot C was involved in both the first and second nitrate injections. The first injection oxidized and removed a substantial fraction of U(IV), so the second injection resulted in oxidation of some of the remaining U(IV). We aimed to investigate how oxidation of U(IV) affected subsequent changes in $\delta^{238}U$ induced by later oxidation of U(IV) by comparing the isotopic change seen in CD-01 of the first experiment to the second year. Documentation of a consistent change in $\delta^{238}U$ would support the use of $\delta^{238}U$ for detecting natural U(IV) oxidation for years following a biostimulation event, despite slow depletion of the solid U(IV) pool.

Groundwater Analyses

All collected groundwater was filtered through 0.45 μm PVDF filters before being preserved by addition of concentrated nitric acid. Groundwater samples were analyzed for $\delta^{238}U$ and dissolved U concentrations on a Nu Plasma HR MC-ICPMS,(26,36) δD on a Los Gatos Research liquid water isotope analyzer,(7) and anion concentrations on a Dionex ion chromatograph(6) (see the Supporting Information for details).

Results

Background Conditions

The upstream well CU-01 provides information about the initial composition of water moving into plot C. In groundwater from well CU-01, nitrate levels remained at background levels (~50 μM) during the 2013 and 2016 oxidation experiments. During the first experiment, δD values of groundwater from well CU-01 did not increase, confirming that amended groundwater did not travel upstream from the injection wells. $\delta^{238}U$ values of this groundwater remained constant at 0.00 ± 0.04‰ despite small seasonal fluctuations in U(VI) concentrations (180 to 210 μg/L) (Table S2).(23) During the second experiment, transient bromide concentration increases (~10% of concentration at injection wells) were observed in CU-01, indicating some

mixing of injected, amended water with upstream groundwater. However, U(VI) concentrations (170 to 180 µg/L) and δ^{238}U values (~0.0‰) of groundwater from CU-01 remained constant (Table S2).

Groundwater in downstream wells was similar isotopically and chemically to upstream well CU-01 before the induced oxidation events, but small differences in U(VI) concentrations and δ^{238}U were observed due to aquifer heterogeneity (Table S2). Prior to the arrival of the first oxidation front, groundwater in the eastern half of plot C in downstream wells CD-18 and CD-01 had marginally lower U(VI) concentrations (~170 and ~180 µg/L, respectively) and δ^{238}U values (~−0.2‰ and ~−0.1‰, respectively) than groundwater from upstream well CU-01 (0.00‰ and ~195 µg/L). Before the second oxidation experiment, groundwater in the eastern half of plot C from well CD-01 had slightly lower U(VI) concentrations (~155 µg/L) and δ^{238}U value (~−0.05‰) than CU-01 (~185 µg/L and 0.0‰). On the western half of plot C, CD-14 appeared to have a slightly higher U(VI) concentration (~200 µg/L) and δ^{238}U value (~0.05‰) compared to those of upstream well CU-01, before the second oxidation experiment. These naturally occurring differences in groundwater chemistry are statistically distinguishable, but they are much smaller than the differences induced by nitrate injection and demonstrate that the groundwater in plot C is nearly homogeneous.

First Oxidation Experiment (2013)

Roughly 4 days after the injection of nitrate and deuterium-enriched groundwater into the eastern half of plot C began, an increase in δD was seen almost simultaneously in monitoring wells CD-18 (~1.0 m downstream of injection wells) and CD-01 (~2.5 m downstream of injection wells). While δD increased significantly, nitrate concentrations remained low, with a maximum concentration of 0.05 mM during the experiment. This indicates near complete reduction of nitrate upstream of these wells. Total dissolved U concentrations began to increase ~4 and ~19 days after the arrival of high-δD injectate in monitoring wells CD-18 and CD-01, respectively (Figure 2).
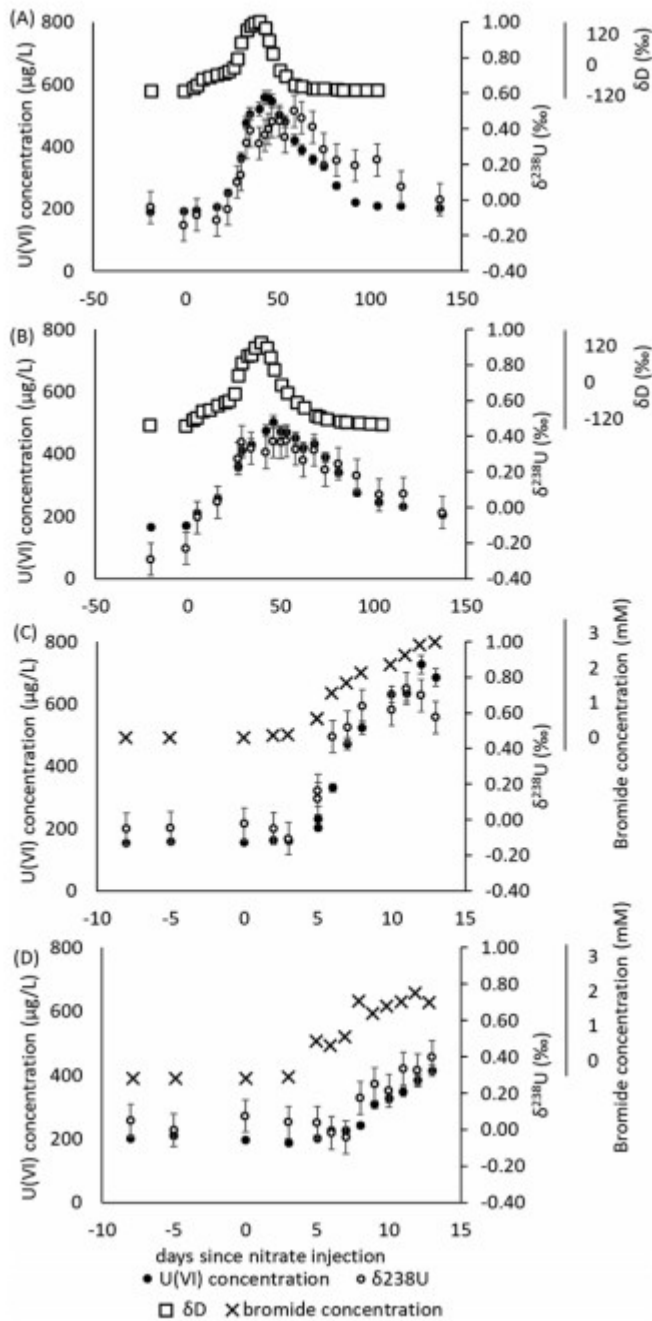
Figure 2. U(VI) concentrations, $\delta^{238}U$, and conservative tracer data (δD or bromide concentrations) for the first and second experiments, respectively over the collection time for all observation wells: (A) CD-01 (more U(VI) and sulfate reduction), 2013 experiment (first oxidation experiment); (B) CD-18 (more U(VI) and sulfate reduction), 2013 experiment (first oxidation experiment); (C) CD-01 (more U(VI) and sulfate reduction), 2016 experiment (second oxidation experiment); (D) CD-14 (less U(VI) and sulfate reduction), 2016 experiment (second oxidation experiment).

On day 23 of the experiment, the injection rate was increased from 36 to 120 mL/min/well to supply more nitrate. Two days later, δD began to increase in monitoring wells CD-18 and CD-01. Dissolved U concentrations increased rapidly ~1 and ~3 days after the arrival of higher δD waters in monitoring

wells CD-18 and CD-01, respectively. Dissolved U concentrations reached a maximum of 503 μg/L in well CD-18 and 558 μg/L in well CD-01 during the experiment. On day 41, δD began to decrease in response to the cessation of nitrate injection 7 days earlier. As δD decreased, dissolved U concentrations began to decrease but remained elevated above 300 μg/L for 88 and 79 days after the injection began in monitoring wells CD-18 and CD-01, respectively (Figure 2).

$\delta^{238}U$ increased as U concentrations increased in monitoring wells CD-18 and CD-01. $\delta^{238}U$ reached a maximum of 0.37‰ in well CD-18 and 0.50‰ in well CD-01 as U concentrations were near their peak (Figure 2). The $\delta^{238}U$ changes in CD-18 reflected the U concentration changes without a significant time lag. In monitoring well CD-01, the $\delta^{238}U$ maximum occurred several days after the concentration maximum, and the subsequent $\delta^{238}U$ decrease appears to lag behind the concentration decrease.

Second Oxidation Experiment (2016)

Four days after the injection of amended groundwater, bromide began to increase in both the eastern and western sides of plot C (Figure 2). Nitrate concentrations increased significantly in groundwater from the western half of plot C in well CD-14, up to 2.0 mM (Figure S1). Using the nitrate-to-bromide ratio, this suggests only 45% of nitrate was reduced on the western half of plot C. In groundwater from the eastern half in well CD-01, nitrate was nearly completely reduced with a maximum concentration of 0.4 mM 7 days after the start of the injection.

Dissolved U concentrations increased concurrently with the arrival of bromide in monitoring wells CD-01 and CD-14 (Figure 2). U concentrations increased steadily to a maximum of 726 μg/L in well CD-01 11 days after the start of injection. U concentrations were still increasing in well CD-14 at the conclusion of sampling with the last sample measured at 415 μg/L. The passing of the oxidation pulse was not measured in this experiment, so bromide and U(VI) concentrations did not decrease at the conclusion of sample collection 12 days after the start of the injection.

$\delta^{238}U$ increased on both sides of plot C as oxidation occurred. In the western half of plot C in well CD-14, $\delta^{238}U$ increased to a maximum of 0.40‰ at high U concentrations 12 days after the start of the injection. In the eastern half of plot C in well CD-01, $\delta^{238}U$ increased consistently in groundwater to a maximum of 0.74‰ (Figure 2) 10 days after the start of the injection.

Discussion

Nitrate Consumption and U(IV) Oxidation

By examining the consumption of nitrate, we estimated how quickly and intensely nitrate affected the aquifer microbial community, which can couple nitrate reduction to release of U and oxidation of other reduced solids such as Fe(II) sulfides. For the east half of plot C, we observed almost complete

consumption of nitrate upstream of monitoring wells CD-01 and CD-18 during the first nitrate injection. The nitrate injection stimulated microbial growth; increases in the number of Fe-oxidizing and S-oxidizing bacteria were observed.[35,37] These microbes appeared to rapidly couple the oxidation of reduced Fe and S phases to the consumption of most of the nitrate.[35] Nitrate removal may also have been coupled to the oxidation of organic carbon.

The nitrate injection also induced remobilization of U, which is evident in increasing dissolved U concentrations in the downstream wells (Figure 2). We believe that the vast majority of this increase was due to U(IV) oxidation. A portion of this increase in dissolved U (defined as U collected through 0.45 μm filters) could be due to release of U(IV)-bearing colloids during the nitrate injection[9,10] (see discussion of impact in the Supporting Information). During our first oxidation experiment, the increase was delayed ~4 and ~19 days in monitoring wells CD-18 and CD-01, respectively, after the arrival of the conservative tracer. After the nitrate injection rate increased, U(VI) concentrations increased significantly ~1 and ~3 days after the arrival of higher concentrations of conservative tracer. This small lag is attributed to adsorption of U(VI) to aquifer solids. The adsorbed U(VI) pool in the aquifer is considerably larger than the dissolved U(VI),[38] and thus downstream advection of U(VI) is anticipated to be retarded relative to advection of nonadsorbing species.[39] During the onset of U(IV) oxidation, as aqueous U(VI) was generated near the injection wells, much of this U(VI) must have adsorbed to aquifer sediments, slowing advection of the U(VI) concentration pulse. A second possible cause of this lag was that microbial oxidation of U(IV) coupled to nitrate reduction did not begin immediately after the start of injection, but rather after growth of nitrate-respiring microbes.

In the second oxidation experiment, the lag was shorter; groundwater U(VI) concentrations increased in wells CD-01 and CD-14 within 3 days (Figure 2). We attribute the difference to the lower initial nitrate injection concentrations used in the first experiment, which would have resulted in slower growth of microbes coupling U(IV) oxidation and nitrate reduction. In addition, more nitrate-respiring microbes were likely available initially in the second experiment for nitrate reduction due to their growth in the initial nitrate amendment.

Comparison of the east and west halves of plot C reveals that less nitrate reduction occurred on the west half of the plot. Only 45% of nitrate was consumed upstream of well CD-14, in contrast with near complete reduction upstream of well CD-01 on the east half. The lower consumption of nitrate on the western half is attributed to the presence of lower quantities of reduced Fe and S phases. This difference is consistent with the plot history, where two successive biostimulation experiments in 2010–11 and 2011–12 impacted the eastern half of the plot, with the 2011–12 experiment being much more intense, whereas only the weaker biostimulation experiment in 2010–11 impacted the western half of the plot.

Amount of U(IV) Oxidized

Using the detailed history of U(VI) concentrations, we can estimate the mass of U(IV) that was oxidized by the first nitrate injection. This, in turn, allows us to examine how the δ^{238}U of U(VI) generated by oxidation of a BRZ varies as the U(IV) is consumed over time. By comparing groundwater U(VI) concentrations from monitoring well CD-01 with those of upstream well CU-01 during the biostimulation experiments and subsequent oxidation experiments, we can estimate the mass of U(IV) deposited during biostimulation and the fraction of total U(IV) lost during the oxidation experiment. We assume that well CU-01 provides a good estimate of the initial composition of upstream groundwater entering plot C and eventually arriving at CD-01. Any difference in concentration is attributed to U(VI) lost from reduction or added from oxidation of U(IV). The mass of U(IV) added or lost, per unit cross-sectional area perpendicular to groundwater flow, can be calculated by

$$U(IV)_{produced} = V_{gw}\varphi \int_{0}^{t_{final}} ([U(VI)]_{CU-01} - [U(VI)]_{CD-01})\, dt \qquad (2)$$

where groundwater velocity (V_{gw}) is 0.5 m/day and porosity (φ) is 0.27.(6) A positive result represents the addition of U(IV) to the aquifer and a negative result represents loss of U(IV). For the two biostimulation events combined (2010–11 and 2011–12), ~5600 mg/m^2 U(IV) was deposited upstream of CD-01. For the first oxidation experiment, ~1970 mg/m^2 was oxidized. Therefore, we estimate that a significant portion, 35%, of U(IV) was oxidized on the east half of plot C in the first oxidation experiment and was not available for the second oxidation experiment. Natural U(IV) oxidation at other times was slow (less than 3 mg/m^2/day), as evidenced by no significant difference between δ^{238}U and U(VI) concentrations of background well CU-01 and monitoring well CD-01.

Adsorption and desorption affect aqueous U(VI) concentrations in CD-01. (7,34) However, there is no net effect on U(VI) concentrations over the course of an entire experiment. During the reduction events, as aqueous U(VI) concentrations decreased, the adsorbed U(VI) would have desorbed and subsequently been reduced and deposited as U(IV). Since this U(VI) was not accounted for in our calculation, we may have underestimated the amount of U(IV) produced during the initial period of biostimulation, as concentrations decreased. However, this unaccounted flux is offset by the recovery phase where aqueous U(VI) concentrations increased back to normal levels and adsorption sites were repopulated with U(VI). Therefore, as long as aqueous U(VI) concentration in CD-01 returned to its prestimulation level after each biostimulation event, the net change in the adsorbed U(VI) pool integrated over the entire experiment should approach zero. The same is true for oxidations events.

While a significant fraction of the previously deposited U(IV) was oxidized during nitrate injections in plot C, U(IV) oxidation rates at other sites may be slower due to differences in the type and amount of reduced solids formed by biostimulation. Research suggests that the crystalline uraninite form of U(IV) is less susceptible to oxidation than noncrystalline U(IV).(40) In biostimulation events similar to those performed at Rifle, CO, the U(IV) generated appears to be a mixture of uraninite and noncrystalline U(IV). (41−46) U(IV) taken from plot C in Rifle, CO, during the biostimulation was approximately one-third uraninite and two-thirds noncrystalline U(IV).(46)The high proportion of noncrystalline U(IV) in plot C makes it more susceptible to oxidation by nitrate than sites dominated by uraninite. In addition, the presence of reduced Fe and S phases can protect U(IV) from oxidation by reacting with and depleting oxidants. If biostimulation occurs at a U-contaminated site with less sulfate reduction occurring, less protective Fe(II) sulfides are produced, possibly allowing for faster rates of U(IV) oxidation.

Determining the $\delta^{238}U$ of Oxidation-Derived U(IV): Application, Assumptions, and Limitations of a Mixing Model

During U(IV) oxidation, increases in $\delta^{238}U$ of U(VI) were seen for all experiments as U(IV) with an elevated $\delta^{238}U$ was released and incorporated into the aqueous U pool. Our experiments at the well-instrumented Rifle site allowed us to estimate the isotopic composition of the oxidized U(IV) and test the hypothesis that U(IV) oxidation induces a consistent increase in $\delta^{238}U$ that can be applied to many U-contaminated sites under a broad range of conditions. We created a simple mixing model to simulate the $\delta^{238}U$ and U(VI) concentrations during mixing of background U(VI) with U(VI) derived from U(IV) oxidization. The model assumes two-component mixing(47) of incoming U(VI) and U(VI) derived from U(IV) oxidation; each component is assumed to have a distinct, unchanging $\delta^{238}U$ value. The model produces a straight mixing line on a plot of $\delta^{238}U$ versus the inverse of U(VI) concentration (Figure 3). Prior to the experiments, the inverse of U(VI) concentration was relatively high with a low $\delta^{238}U$. We assume an unchanging $\delta^{238}U$ value of incoming U(VI), but changes in groundwater flow and geochemistry (such as prolonged U(VI) reduction) could have induced small changes in $\delta^{238}U$ of incoming U(VI) (see the Supporting Information for details). As U(VI) was added by U(IV) oxidation, the inverse of U(VI) concentration decreased and $\delta^{238}U$ increased. The data from each well during each experiment conform to a straight line; we found best-fit lines using standard linear regression. The y-intercept of each fit line represents the $\delta^{238}U$ value of the mobilized U(IV). If no isotopic fractionation occurred during U(IV) oxidation, this $\delta^{238}U$ value is also the calculated isotopic composition of the solid U(IV).
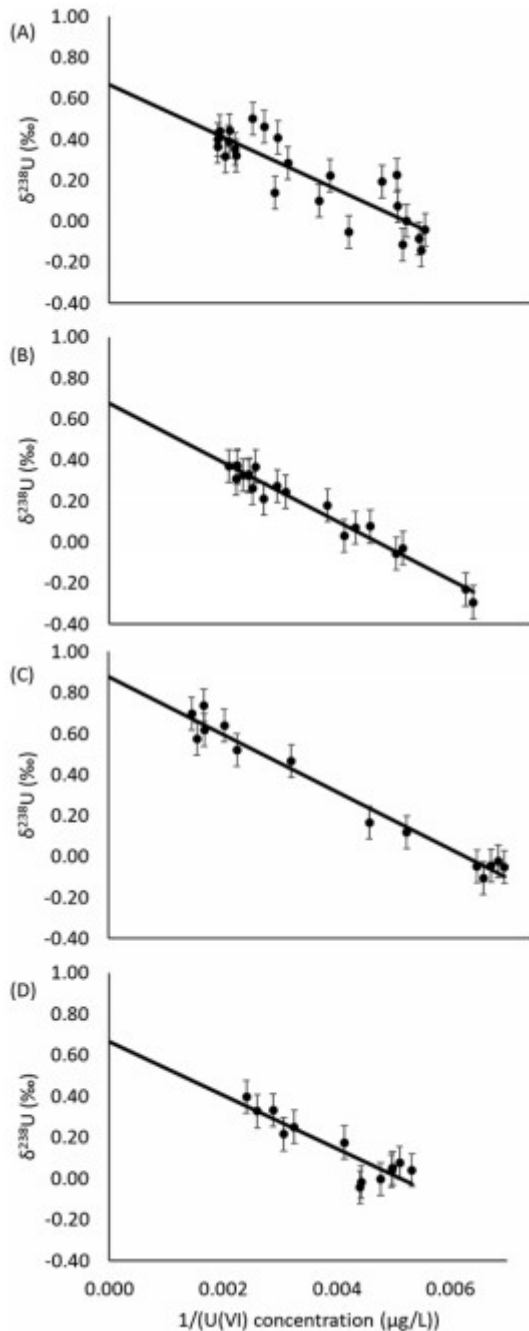
Figure 3. δ^{238}U vs inverse of dissolved U concentration during the oxidation experiments: (A) well CD-01 (more U(VI) and sulfate reduction) during the first oxidation experiment; (B) CD-18 (more U(VI) and sulfate reduction), first oxidation experiment; (C) CD-01 (more U(VI) and sulfate reduction), second oxidation experiment; (D) CD-14 (less U(VI) and sulfate reduction), second oxidation experiment.

This mixing model does not incorporate the effects of U(VI) adsorption/desorption, which is known to produce small shifts in δ^{238}U values. (26−29) Because of the strong influence of U(VI) adsorption, we cannot utilize δ^{238}U to accurately calculate the rate of U(IV) oxidation without use of reactive transport modeling, but simple corrections may be applied to

estimate $\delta^{238}U$ of released U(IV). As oxidation of U(IV) occurs, much of the excess aqueous U(VI) adsorbs to aquifer minerals. Since ^{235}U adsorbs preferentially, $\delta^{238}U$ of aqueous U(VI) increases more than would be expected by U(IV) oxidation alone in the absence of adsorption. Because of this unaccounted increase in $\delta^{238}U$ of aqueous U(VI) during U(IV) oxidation, the simple mixing model overestimates $\delta^{238}U_{U(IV)}$. However, this effect can be readily corrected, provided the proportions of aqueous and adsorbed U(VI) remain constant during the addition of U(VI) from U(IV) oxidation. The data remain on a straight mixing line, but the y-intercept is shifted higher. The resulting overestimation of $\delta^{238}U_{U(IV)}$ (Figure S2) may be calculated as

$$\delta^{238}U_{U(IV),aq} - \delta^{238}U_{U(IV),true} = -\Delta^{238}U_{ads}f_{ads} \qquad (3)$$

where $\delta^{238}U_{U(IV),aq}$ is the y-intercept of the data fit line without incorporating U(VI) adsorption, $\delta^{238}U_{U(IV),true}$ is the true $\delta^{238}U_{U(IV)}$ incorporating U(VI) adsorption, $\Delta^{238}U = \delta^{238}U_{adsorbed\ U(VI)} - \delta^{238}U_{aqueous\ U(VI)}$, and f_{ads} is the fraction of U(VI) in a given aquifer volume that is adsorbed to aquifer sediments, out of the total pool, adsorbed and dissolved.

Using a $\Delta^{238}U$ of −0.20‰ and f_{ads} of 0.94 consistent with the Rifle site,[29,38] the simple mixing model overestimated $\delta^{238}U_{U(IV)}$ by ~0.19‰. Applying this correction to the y-intercepts of the aqueous U(VI) data, we obtained a narrow range for the true $\delta^{238}U$ value of released U(IV). $\delta^{238}U_{U(IV)}$ is calculated at 0.49‰ for CD-18 and 0.48‰ for CD-01 in the 2013 experiment and 0.69‰ for CD-01 and 0.47‰ for CD-14 in 2016 (Figure 3).

The simple mixing model of background U(VI) and oxidized U(IV) did not include isotopic heterogeneity of U(IV), which likely factored into the U(IV) oxidation experiments. $\delta^{238}U$ of U(IV) within the BRZ can vary due to differences in aquifer permeability, which can control groundwater velocity, aqueous U concentrations, and U(VI) reduction rate.[32] In addition, U(VI) reduction is predicted to generate isotopic heterogeneity of U(IV) within the BRZ with predicted lower $\delta^{238}U$ values (up to ~2‰ lower) farther downstream from the injection wells (see the Supporting Information for details). If oxidation of this U(IV) occurred, a much smaller increase (or even a decrease) in $\delta^{238}U$ of U(VI) could occur. After ~35% of the U(IV) was oxidized in the first experiment in the eastern half of plot C, the $\delta^{238}U$ signal of the same section in the second experiment was similar, suggesting that a large proportion of U(IV) must be oxidized before a significant change in $\delta^{238}U$ of released U. The consistent increase in $\delta^{238}U$ during our oxidation experiments appears to demonstrate that assuming an unchanging $\delta^{238}U$ is reasonable. Most data fit a simple mixing line, suggesting the dominance of U(IV) oxidation on our collected data.

If a portion of the increase in dissolved U was due to release of U(IV)-bearing colloids, aqueous U concentrations and $\delta^{238}U$ would still increase concurrently, signaling the release of U(IV) from the sediment. The good fit of the simple two-component mixing model suggests either that the colloidal

U(IV) component is small or that its isotopic composition matches that of the U released by oxidation (see the Supporting Information for details).

Despite differences in aquifer conditions, the calculated isotopic signature of U(IV) for all monitored wells was fairly consistent: 0.48‰, 0.49‰, 0.69‰, and 0.47‰ for groundwater from wells CD-01 and CD-18 during the first experiment and wells CD-01 and CD-14 during the second experiment, respectively. Different biostimulation conditions as well as prior oxidation events had only small effects on the δ^{238}U of the remobilized U(IV). These results support the use of δ^{238}U to detect U(IV) oxidation following biostimulation. However, due to the significant uncertainty provided by complications of U(VI) adsorption, U(VI) reduction, isotopic heterogeneity of U(IV), and U(IV) colloids (explained further in the Supporting Information), determinations of the amount of U(IV) release are semiquantitative.

Environmental Implications

During our oxidation experiments, a significant increase in δ^{238}U (~0.4‰) was observed. The high δ^{238}U values consistently observed during U(IV) oxidation in these experiments confirms that δ^{238}U may be useful in detecting remobilization of U(IV) previously sequestered by reduction of dissolved U(VI). However, natural U(IV) oxidation by various oxidants is expected to occur significantly slower with smaller increases in δ^{238}U. In some cases, the oxidation-induced increase in δ^{238}U may not be resolvable from the background. For example, if U(IV) oxidation increases U(VI) concentrations by only 15%, an increase in δ^{238}U of ~0.1‰ would be expected. Given the uncertainties of our isotopic measurements (±0.08‰), this increase in δ^{238}U may not be distinguishable from background U(VI). Higher precision measurements (<0.05‰ uncertainty has been reported elsewhere)(48,49) should improve this situation. Uncertainty could also be improved by averaging of multiple measurements. For example, natural oxidation may be detectable by taking the standard error of several temporally similar δ^{238}U measurements under similar redox conditions and comparing these to samples from a different period when redox conditions are different. However, the utility of this method is limited for slow oxidation, over periods of years.

Our results demonstrate that rapid release of U from oxidation by nitrate can be detected by measurement of groundwater δ^{238}U upstream and downstream of a BRZ. The large number of wells at the Rifle site allowed us to track a concurrent increase in U(VI) concentrations and ^{238}U/^{235}U ratios in downstream wells as U(IV) is oxidized from the BRZ. In this well-instrumented setting, the δ^{238}U method for detecting oxidation could be viewed as redundant. However, many sites have a much lower density of wells and have poorly defined flow paths. An increase in U(VI) concentrations in a downstream well at one of these sites could be due to a change in groundwater source or desorption. In such cases, the isotopic approach likely provides better evidence of U(IV) oxidation because it is a more direct

indicator of oxidation. A strong increase in $\delta^{238}U$ relative to the site background indicates release of high-$\delta^{238}U$ U(IV).

This isotopic method of detecting oxidation should be applicable to other redox-sensitive elements, such as selenium and chromium. These elements isotopically fractionate during reduction,(50−53) so oxidation and remobilization of their reduced phases is expected to isotopically shift the measured aqueous pool. Unambiguous detection of remobilization of these toxic contaminants through isotope ratios could allow for more rapid employment of remedial actions.

References

(1) Gavrilescu, M.; Pavel, L. V.; Cretescu, I. Characterization and remediation of soils contaminated with uranium. J. Hazard. Mater. 2009, 163, 475−510. (2) Riley, R. G.; Zachara, J. M.; Wobber, F. J. Chemical contaminants on DOE lands and selection of contaminant mixtures for subsurface science research. DOE, 1992. (3) Abdelouas, A. Uranium mill tailings: geochemistry, mineralogy, and environmental impact. Elements 2006, 2, 335−341. (4) Wall, J. D.; Krumholz, L. R. Uranium reduction. Annu. Rev. Microbiol. 2006, 60, 149−166. (5) Anderson, R. T.; Vrionis, H. A.; Ortiz-Bernad, I.; Resch, C. T.; et al. Stimulating the in situ activity of Geobacter species to remove uranium from the groundwater of a uranium-contaminated aquifer. Appl. Environ. Microbiol. 2003, 69, 5884−5891. (6) Williams, K. H.; Long, P. E.; Davis, J. A.; Wilkins, M. J.; et al. Acetate Availability and its Influence on Sustainable Bioremediation of Uranium-Contaminated Groundwater. Geomicrobiol. J. 2011, 28, 519− 539. (7) Long, P. E.; Williams, K. H.; Davis, J. A.; Fox, P. M.; et al. Bicarbonate impact on U (VI) bioreduction in a shallow alluvial aquifer. Geochim. Cosmochim. Acta 2015, 150, 106−124. (8) Istok, J. D.; Senko, J. M.; Krumholz, L. R.; Watson, D.; Bogle, M. A.; et al. In Situ Bioreduction of Technetium and Uranium in a Nitrate-Contaminated Aquifer. Environ. Sci. Technol. 2004, 38, 468− 475. (9) Thompson, A.; Chadwick, O. A.; Boman, S.; Chorover, J. Colloid Mobilization During Soil Iron Redox Oscillations. Environ. Sci. Technol. 2006, 40, 5743−5749. (10) Wang, Y.; Frutschi, M.; Suvorova, E.; Phrommavanh, V.; Descostes, M.; Osman, A. A.; Geipel, G.; Bernier-Latmani, R. Mobile uranium(IV)-bearing colloids in a mining-impacted wetland. Nat. Commun. 2013, 4, 2942. (11) Moon, H. S.; Komlos, J.; Jaffe, P. R. Biogenic U(IV) oxidation by dissolved oxygen and nitrate in sediment after prolonged U(VI)/ Fe(III)/SO42− reduction. J. Contam. Hydrol. 2009, 105, 18−27. (12) Bi, Y.; Hyun, S. P.; Kukkadapu, R. K.; Hayes, K. F. Oxidative dissolution of UO2 in a simulated groundwater containing synthetic nanocrystalline mackinawite.

Geochim. Cosmochim. Acta 2013, 102, 175−190. (13) Bi, Y.; Hayes, K. F. Nano-FeS Inhibits UO2 Reoxidation under Varied Oxic Conditions. Environ. Sci. Technol. 2014, 48, 632−640. (14) Carpenter, J.; Bi, Y.; Hayes, K. F. Influence of Iron Sulfides on Abiotic Oxidation of UO2 by Nitrite and Dissolved Oxygen in Natural Sediments. Environ. Sci. Technol. 2015, 49, 1078−1085. (15) Paradis, C. J.; Jagadamma, S.; Watson, D. B.; McKay, L. D.; Hazen, T. C.; et al. In situ mobility of uranium in the presence of nitrate following sulfate-reducing conditions. J. Contam. Hydrol. 2016, 187, 55−64. (16) Senko, J. M.; Istok, J. D.; Suflita, J. M.; Krumholz, L. R. In-Situ Evidence for Uranium Immobilization and Remobilization. Environ. Sci. Technol. 2002, 36, 1491−1496. (17) Beller, H. R. Anaerobic, Nitrate-Dependent Oxidation of U(IV) Oxide Minerals by the Chemolithoautotrophic Bacterium Thiobacillus denitrificans. Appl. Environ. Microbiol. 2005, 71, 2170−2174. (18) Moon, H. S.; Komlos, J.; Jaffe, P. R. Uranium Reoxidation in Previously Bioreduced Sediment by Dissolved Oxygen and Nitrate. Environ. Sci. Technol. 2007, 41, 4587−4592. (19) Jaffey, A. H.; Flynn, K. F.; Glendenin, L. E.; Bentley, W. C.; Essling, A. M. Precision measurement of half-lives and specific activities of 235U and 238U. Phys. Rev. C: Nucl. Phys. 1971, 4, 1889− 1906. (20) Basu, A.; Sanford, R. A.; Johnson, T. M.; et al. Uranium isotopic fractionation factors during U (VI) reduction by bacterial isolates. Geochim. Cosmochim. Acta 2014, 136, 100−113. (21) Stylo, M.; Neubert, N.; Wang, Y.; Monga, N.; Romaniello, S. J.; Weyer, S.; Bernier-Latmani, R. Uranium isotopes fingerprint biotic reduction. Proc. Natl. Acad. Sci. U. S. A. 2015, 112, 5619−5624. (22) Stirling, C. H.; Andersen, M. B.; Warthmann, R.; Halliday, A. N. Isotope fractionation of 238U and 235U during biologically-mediated uranium reduction. Geochim. Cosmochim. Acta 2015, 163, 200−218. (23) Shiel, A. E.; Johnson, T. M.; Lundstrom, C. C.; Laubach, P. G.; Long, P. E.; Williams, K. H. Reactive transport of uranium in a groundwater bioreduction study: Insights from high-temporal resolution 238U/235U data. Geochim. Cosmochim. Acta 2016, 187, 218−236. (24) Stirling, C. H.; Andersen, M. B.; Potter, E.; Halliday, A. N. Lowtemperature isotopic fractionation of uranium. Earth Planet. Sci. Lett. 2007, 264, 208−225. (25) Brown, S. T.; Basu, A.; Ding, X.; Christensen, J. N.; DePaolo, D. J. Inorganic Uranium Isotope Fractionation is Dependent on Aqueous Speciation. Goldschmidt Abs. 2017, 7a. (26) Weyer, S.; Anbar, A. D.; Gerdes, A.; Gordon, G. W.; Algeo, T. J.; Boyle, E. A. Natural fractionation of 238U/235U. Geochim. Cosmochim. Acta 2008, 72, 345−359. (27) Brennecka, G. A.; Wasylenki, L. E.; Bargar, J. R.; Weyer, S.; Anbar, A. D. Uranium Isotope Fractionation during Adsorption to Mn-Oxyhydroxides. Environ. Sci. Technol. 2011, 45, 1370−1375. (28) Goto, K. T.; Anbar, A. D.; Gordon, G. W.; Romaniello, S. J.; Shimoda, G.; et al. Uranium isotope systematics of ferromanganese crusts in the Pacific Ocean: Implications for the marine 238U/235U isotope system. Geochim. Cosmochim. Acta 2014, 146, 43−58. (29) Jemison, N. E.; Johnson, T. M.; Shiel, A. E.; Lundstrom, C. C. Uranium Isotopic Fractionation Induced by U(VI) Adsorption onto Common Aquifer Mineral. Environ. Sci. Technol. 2016, 50, 12232− 12240. (30) Wang, X.; Johnson, T. M.; Lundstrom, C. C. Isotope fractionation during oxidation of

tetravalent uranium by dissolved oxygen. Geochim. Cosmochim. Acta 2015, 150, 160−170. (31) Wainwright, H. M.; Orozco, A. F.; Bucker, M.; Dafflon, B.; et al. Hierarchical Bayesian method for mapping biogeochemical hot spots using induced polarization imaging. Water Resour. Res. 2016, 52, 533− 551. (32) Li, L.; Gawande, N.; Kowalsky, M. B.; Steefel, C. I.; Hubbard, S. S. Physicochemical Heterogeneity Controls on Uranium Bioreduction Rates at the Field Scale. Environ. Sci. Technol. 2011, 45, 9959−9966. (33) Bao, C.; Wu, H.; Li, L.; Newcomer, D.; Long, P. E.; Williams, K. H. Uranium Bioreduction Rates across Scales: Biogeochemical Hot Moments and Hot Spots during a Biostimulation Experiment at Rifle, Colorado. Environ. Sci. Technol. 2014, 48, 10116−10127. (34) Shiel, A. E.; Laubach, P. G.; Johnson, T. M.; Lundstrom, C. C.; Long, P. E.; Williams, K. H. No Measurable Changes in 238U/235U due to Desorption−Adsorption of U(VI) from Groundwater at the Rifle, Colorado, Integrated Field Research Challenge Site. Environ. Sci. Technol. 2013, 47, 2535−2541. (35) Jewell, T. N. M.; Karaoz, U.; Brodie, E. L.; Williams, K. H.; Beller, H. R. Metatranscriptomic evidence of pervasive and diverse chemolithoautotrophy relevant to C, S, N and Fe cycling in a shallow alluvial aquifer. ISME J. 2016, 10, 2106−2117. (36) Bopp, C. J.; Lundstrom, C. C.; Johnson, T. M.; et al. Uranium 238U/ 235U isotope ratios as indicators of reduction: results from an in situ biostimulation experiment at Rifle, Colorado, USA. Environ. Sci. Technol. 2010, 44, 5927−5933. (37) Bosch, J.; Lee, K.-Y.; Jordan, G.; Kim, K.-W.; Meckenstock, R.- U. Anaerobic, Nitrate-Dependent Oxidation of Pyrite Nanoparticles by Thiobacillus denitrificans. Environ. Sci. Technol. 2012, 46, 2095−2101. (38) Fox, P. M.; Davis, J. A.; Hay, M. B.; Conrad, M. E.; et al. Ratelimited U(VI) desorption during a small-scale tracer test in a heterogeneous uranium-contaminated aquifer. Water Resour. Res. 2012, 48, W05512. (39) Freeze, R. A.; Cherry, J. A. Groundwater Contamination. In Groundwater; Prentice-Hall, Inc.: Englewood Cliffs, NJ, 1979; pp 403− 408. (40) Cerrato, J. M.; Ashner, M. N.; Alessi, D. S.; Lezama-Pecheco, J. S.; Bernier-Latmani, R.; et al. Relative Reactivity of Biogenic and Chemogenic Uraninite and Biogenic Noncrystalline U(IV). Environ. Sci. Technol. 2013, 47, 9756−9763. (41) Schofield, E. J.; Veeramani, H.; Sharp, J. O.; Suvorova, E.; Bernier-Latmani, R.; et al. Structure of biogenic uraninite produced by Shewanella oneidensis strain MR-1. Environ. Sci. Technol. 2008, 42, 7898−7904. (42) Bernier-Latmani, R.; Veeramani, H.; Dalla Vecchia, E.; Junier, P.; Lezama-Pacheco, J. S.; et al. Non-uraninite products of microbial U(VI) reduction. Environ. Sci. Technol. 2010, 44, 9456−9462. (43) Fletcher, K. E.; Boyanov, M. I.; Thomas, S. H.; Wu, Q.; Kemner, K. M.; Löffler, F. E. U(VI) reduction to mononuclear U(IV) by Desulfitobacterium species. Environ. Sci. Technol. 2010, 44, 4705− 4709. (44) Boyanov, M. I.; Fletcher, K. E.; Kwon, M. J.; Rui, X.; O'Loughlin, E. J.; et al. Solution and microbial controls on the formation of reduced U(VI) species. Environ. Sci. Technol. 2011, 45, 8336−8344. (45) Stylo, M.; Alessi, D. S.; Shao, P. P.; Lezama-Pacheco, J. S.; Bargar, J. R.; Bernier-Latmani, R. Biogeochemical Controls on the Product of Microbial U(VI) Reduction. Environ. Sci. Technol. 2013, 47, 12351−12358. (46) Alessi, D. S.; Lezama-Pecheco, J. S.; Janot, N.; Suvorova, E. I.; Cerrato, J.

M.; et al. Speciation and Reactivity of Uranium Products Formed during in Situ Bioremediation in a Shallow Alluvial Aquifer. Environ. Sci. Technol. 2014, 48, 12842−12850. (47) Faure, G. Principles of Isotope Geology, 2nd ed.; John Wiley and Sons Inc.: New York, 1986. (48) Dahl, T. W.; Boyle, R. A.; Canfield, D. E.; Connelly, J. N.; et al. Uranium isotopes distinguish two geochemically distinct stages during the later Cambrian SPICE event. Earth Planet. Sci. Lett. 2014, 401, 313−326. (49) Andersen, M. B.; Elliott, T.; Freymuth, H.; Sims, K. W. W.; Niu, Y.; Kelley, K. A. The terrestrial uranium isotope cycle. Nature 2015, 517, 356−359. (50) Herbel, M. J.; Johnson, T. M.; Oremland, R. S.; Bullen, T. D. Fractionation of selenium isotopes during bacterial respiratory reduction of selenium oxyanions. Geochim. Cosmochim. Acta 2000, 64, 3701−3709. (51) Ellis, A. S.; Johnson, T. M.; Bullen, T. D. Chromium Isotopes and the Fate of Hexavalent Chromium in the Environment. Science 2002, 295, 2060−2062. (52) Johnson, T. M.; Bullen, T. D. Selenium isotope fractionation during reduction by Fe(II)-Fe(III) hydroxide-sulfate (green rust). Geochim. Cosmochim. Acta 2003, 67, 413−419. (53) Basu, A.; Johnson, T. M.; Sanford, R. A. Cr isotope fractionation factors for Cr(VI) reduction by a metabolically diverse group of bacteria. Geochim. Cosmochim. Acta 2014, 142, 349−361.